Chapter

Microfluidic Adsorption-Based Biosensors: Mathematical Models of Time Response and Noise, Considering Mass Transfer and Surface Heterogeneity

Ivana Jokić

Abstract

Adsorption-based microfluidic sensors are promising tools for biosensing. Advanced mathematical models of time response and noise of such devices are needed in order to improve the interpretation of measurement results, and to achieve the optimal sensor performance. Here the mathematical models are presented that take into account the coupling of processes that generate the sensor signal: adsorption–desorption (AD) of the target analyte particles on the heterogeneous sensing surface, and mass transfer (MT) in a microfluidic chamber. The response kinetics and AD noise (which determines the ultimate sensing performance) of protein biosensors are analyzed, assuming practically relevant analyte concentrations, sensing surface areas and MT parameters. The condition is determined under which MT significantly influences the sensor characteristics relevant for reliable analyte detection and quantification. It is shown that the development of improved mathematical models of sensor temporal response and noise can be used as one of strategies for achieving better sensing performance.

Keywords: microfluidic biosensor, surface heterogeneity, mass transfer, adsorption–desorption noise, mathematical model

1. Introduction

Microfluidic adsorption-based biosensors are promising devices for real-time, in-situ and low-cost analysis of samples taken from the environment, food or living organisms, enabling detection of the presence and measurement of the amount of target biological specimens: biomolecules (such as proteins or DNA fragments), microorganisms, or other biological structures [1–3]. Such sensors are highly sensitive, capable of operation with small sample quantities, and also small, lightweight and energy efficient, thus being especially suitable for autonomuous, portable and distributed sensing applications [4–6]. Due to such characteristics, development of microfluidic sensors is very significant for environmental protection, medicine, agriculture, food inspection, public healthcare and security, and other fields, where they can substitute large and expensive laboratory equipment, typically located far

from the place where the samples are taken for the analysis. They also enable the development of new fields of biosensor applications, such as the personalized medical point-of-care diagnostics, telemedicine, wearable sensors etc. [7–9].

In order to utilize the great potential of adsorption-based microfluidic biosensors for practical applications, research is performed aiming to enable optimization of their performance. The increase of sensitivity and response rate of the sensors, better selectivity, lowering of the minimal detectable concentration, higher reliability of measurement results ant their more accurate interpretation, as well as the research and development of new measurement methods, which enable obtaining of more information about one or multiple adsorbed substances at the same time, are of great practical significance. In that sense, of particular interest is to know the dependence of the temporal response and the sensor noise on the parameters of the sensing element, the measurement system, and the experimental conditions, which requires the development and application of mathematical models that take into account physical processes and phenomena relevant for generating the response and its fluctuations. The adsorption and desorption (AD) processes are inevitably taken into account in modeling of the response and noise, since they are fundamental for sensor operation, and are also the source of adsorption–desorption noise, which sets the fundamental limits of detection and quantification of the analyte. In structures of micrometer and nanometer dimensions, AD noise can dominantly determine the values of minimal detectable and quantifiable signal, as well as other limiting sensor performances, especially in the case of low analyte concentration [10–20]. In various cases, apart from the AD process of the target analyte, different additional processes influence the sensor response kinetics and noise, so it is necessary to take them into account in mathematical models.

The objective of this work is to present mathematical models of the temporal response and adsorption–desorption noise of microfluidic adsorption-based biosensors, that take into account the processes responsible for the generation of the sensor signal: adsorption–desorption of the target analyte particles on the heterogeneous sensing surface, and mass transfer (MT) in a microfluidic chamber. Section 2 presents the mathematical models of the sensor temporal response, while Section 3 describes the AD noise models, developed for the cases considered in Section 2. In Section 4, the results will be presented of the temporal response analysis, and of the analysis of AD noise of protein biosensors, both performed by using of the models presented in Sections 2 and 3, assuming practically relevant analyte concentrations, sensing surface areas and MT parameters. The conclusions will be summarized in Section 5.

2. Mathematical models of sensor temporal response

In adsorption-based biosensors (e.g. SPR (*Surface Plasmon Resonance*), resistive graphene-based, CNT (*Carbon NanoTube*) or NWFET (*NanoWire Field Effect Transistor*), SAW (Surface Acoustic Wave), FBAR (*thin Film Bulk Acoustic wave Resonator*), microcantilever sensors) detection of the target analyte and measurement of its concentration are based on the change of a measurable parameter of the sensing element, caused by analyte adsorption on the active surface [21–28]. Namely, the adsorption leads to the change of some of the sensing element's physical parameters (e.g. the mechanical strain or mechanical structure's mass, the effective density of the surface layer or its conductivity, the refraction index, the distribution of electric charges on the surface), which changes at least one measurable parameter of the sensor (e.g. the deflection or the resonant frequency of the mechanical structure; the amplitude, frequency or phase of surface or bulk acoustic

waves in mechanical sensors; the resistance or current in electrical sensors; the intensity, reflection, transmission, or absorption of light in optical sensors).

Here, the term "temporal response of adsorption-based sensors" will be used to denote the temporal change of a certain physical parameter of the sensing element, which is induced by analyte adsorption. At any given time, that change is determined by the number of analyte particles bound to the sensing surface, and that number depends on the target analyte concentration in the sample. This enables the measurement of the concentration of the target substance to be performed by measuring the change of the physical parameter. Therefore, the mathematical model of the sensor temporal response is based on the model of the time evolution of the number of adsorbed particles as a function of analyte concentration, assuming that there is a known (preferably linear) relation between the two quantities.

In the analyses of microfluidic biosensors time response, which have been published in the literature, it is often assumed that the change of the number of adsorbed particles occurs only due to the AD process of the target substance, and the interpretation of experimental results is performed according to that [29, 30]. This simplified interpretation of the events occurring on the sensing surface is justified under the conditions that ensure a negligible influence of other processes, and assume a homogeneous adsorption surface. Analyses that include some of the additional effects that also influence the current number of adsorbed target particles are less abundant in the existing literature. For example, the mass transfer process of target adsorbate particles in a reaction chamber, toward or away from adsorption sites on the sensing surface, coupled with the AD process, is considered in [31–33]. Competitive AD processes of target and competitor substances are analyzed in [34, 35]. An example of the analysis encompassing multiple phenomena is the research of adsorption processes of two or three analytes on the surface of the same sensor, coupled with mass transfer processes of corresponding particles [36–38]. Sensing surface heterogeneity and mass transfer processes in biosensors are considered within the analysis of sensor models response in [30, 36, 39], where the need is emphasized for taking into account both of these factors simultaneously while creating experiments and interpreting the measurement results.

In this section, first the starting system of equations will be presented that model the change of the number of adsorbed particles on a sensing surface with an arbitrary number of different adsorption sites, and take into account mass transfer processes of analyte particles in the sensor chamber. Subsequently, simplified physical models will be defined and presented by suitable equations for certain cases of practical significance, in a similar way as in [39]. Also, conditions will be defined under which the application of the approximate models is justified. The case of adsorbing surface with two types of adsorption sites will be particularly considered.

2.1 Starting equations

It is assumed that the sensing element of a sensor is in a microfluidic reaction chamber of a rectangular cross-section, with the sample to be analyzed flowing through it. In **Figure 1** (left) a schematic representation is given of the chamber and the sensing element, with the designations of dimensions and coordinate axes. During the laminar fluid flow, a parabolic velocity profile is formed in the chamber (the profile belongs to the z = const. plane, and it is constant in the z-axis direction in the adsorbing surface zone).

On the sensor's active surface the recognition and binding of the target analyte occurs. Adsorption–desorption and mass transfer are the key processes for binding of particles to the sensing surface. The former is the process of binding of the

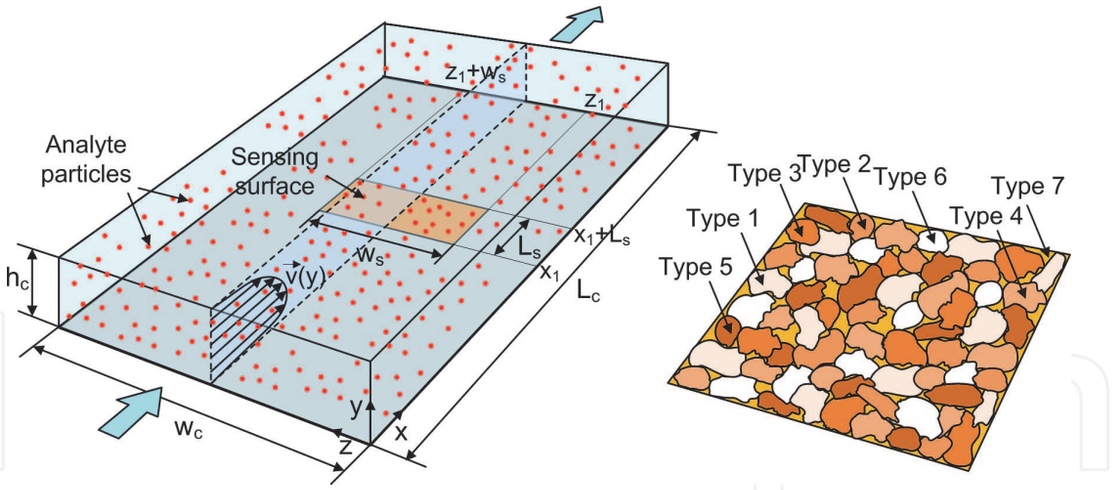

Figure 1.
Left: Schematic representation of a sensor flow-through reaction chamber of rectangular cross-section: geometry of the system with designations of dimensions and coordinate axes. The shaded longitudinal section in the z = *const. plane, whose boundaries are denoted by a dashed line, shows the convection velocity profile (the case of laminar fluid flow). Right: Part of the heterogeneous sensing surface that contains multiple (e.g. 7, as shown) types of adsorption sites of different affinities toward the target analyte.*

analyte particles to surface adsorption sites due to a certain affinity, and unbinding from them. The latter encompasses the processes (convection and diffusion) by which the analyte particles are transported through the microfluidic chamber to or from the binding sites. The coupling of these processes determines the spatial and temporal dependence of the analyte concentration in the chamber.

In the analysis, it is assumed that the adsorption occurs in a single layer only, that only one analyte particle can be adsorbed on an adsorption site, and that the probability of adsorption on any given site (or desorption from it), does not depend on the occupancy of adjacent sites. In the case of a homogeneous sensing surface (in the sense of the affinity toward the target analyte particles), the AD process is characterized by a single pair of adsorption and desorption rate constants, k_a and k_d.

The active surface of affinity-based sensors is often not comprised of uniform adsorption sites to which the particles of the target analyte bind [30, 40]. The reason for this can be a non-uniform surface morphology or chemical composition, or the existence of multiple possible binding sites for analyte particles due to the material structure on the molecular scale. In more detail, the presence of various defects, irregularities, cavities, pores, impurities, contaminants, different functional groups on the surface, etc. are some of numerous features that constitute the surface heterogeneity. Materials in the form of flakes with specific binding sites on edges and basal planes, such as liquid-phase exfoliated graphene [41], are also an example of a heterogeneous sensing surface. When a surface is functionalized with specific capturing probes for the target analyte, adsorption sites heterogeneity can be manifested through nonspecific binding of analyte particles to the surface. An adsorption surface can also be heterogeneous due to uneven binding of functionalizing entities (e.g. non-uniform orientation of capturing proteins when attached to the surface), which influences the affinity toward the analyte, and the efficiency of its binding. Whatever the reason, a heterogeneous sensing surface can be characterized by different affinities of different surface sites for the analyte particles binding. The analyte's AD process is then characterized by a certain distribution of adsorption and desorption rate constants across the surface, and it is described by a model that takes into account the surface non-uniformity.

If we assume that there is n types of adsorption sites on the surface, the surface heterogeneity can be described by a discrete set of n values of adsorption energies

for the given analyte, thus yielding n pairs of adsorption and desorption rate constants (k_{ai}, k_{di}), $i = 1,2 \ldots n$. Adsorption of a single analyte on n types of adsorption sites, randomly distributed across the adsorbing surface of a microfluidic sensor, is mathematically described by $n + 1$ equations, and by boundary and initial conditions. One of the equations is the convection-diffusion equation (for a microfluidic chamber of a rectangular cross-section, whose illustration is shown in **Figure 1** (left))

$$\frac{\partial C}{\partial t} = -v\frac{\partial C}{\partial x} + D\left(\frac{\partial^2 C}{\partial x^2} + \frac{\partial^2 C}{\partial y^2} + \frac{\partial^2 C}{\partial z^2}\right) \tag{1}$$

Here, D is the diffusion coefficient of analyte particles, and v is the flow velocity of the sample. The remaining n equations pertain to the processes of reversible binding of particles to adsorption sites of different types. Each of these processes, which are coupled in a general case, can be regarded as one of n components of a complex AD process. It is known that the Langmuir adsorption model assumes the uniformity of adsorption sites. In the case of heterogeneous surface sites, it can be assumed that the adsorbent surface consists of a collection of locally homogeneous surfaces, and that the adsorption on each of them can be considered as Langmuir adsorption. All the parts of the sensing surface S with the adsorption sites of the type i, constitute the surface S_i of area A_i. The above-mentioned set of n equations can thus be written as

$$\begin{aligned} &\frac{\partial \eta_i}{\partial t} = k_{ai}C_S\left(\eta_{\max,i} - \eta_i\right) - k_{di}\eta_i, \quad (x,0,z) \in S_i \\ &\eta_i = 0 \qquad\qquad\qquad\qquad\qquad\quad , \quad (x,0,z) \notin S_i \end{aligned}, i = 1,2 \ldots n \tag{2}$$

Here η_i is the surface density of the analyte particles adsorbed on sites of the i^{th} type, $\eta_{max,i}$ is the surface density of adsorption sites of the matching kind, and C_s is the analyte concentration adjacent to the sensing surface. It is assumed that the adsorption sites are uniformly distributed across the surface S_i, so $\eta_{max,i}$ does not depend on the coordinates x and z.

The boundary and initial conditions are as follows: 1. at the entrance of the chamber ($x = 0$) the concentration is equal to that in the analyzed sample: $C(t,0,y,z) = C_0$; 2. at the exit from the chamber the continuity condition assumes free convection: $\partial C/\partial x = 0$ for $x = L_c$; 3. the initial adsorbate particle distribution in the chamber is uniform: $C(0,x,y,z) = C_0$, 4. in the zone of the sensing element, which is defined by the coordinates $y = 0$, $x_1 \le x \le x_1 + L_s$, $z_1 \le z \le z_1 + w_s$ (L_s is the adsorption zone length, and w_s is its width), there is a balance between the diffusion flux in the direction perpendicular to the surface, and the net adsorption rate per unit surface

$$D\frac{\partial C}{\partial y}\bigg|_{(t,x,0,z)} = k_{ai}C_s\left(\eta_{\max,i} - \eta_i\right) - k_{di}\eta_i, i = 1, 2, \ldots, n \tag{3}$$

The i^{th} Eq. (3) is valid on the parts of adsorbing surface with the adsorption sites of the i^{th} type; on the remaining part of the chamber's surface where $y = 0$, and on the whole chamber's surface where $y = h_c$, the zero flux condition is valid; 5. on the edges of every adsorption zone the flux equals zero (the adsorbed particles leave the adsorbing zone only by desorption); 6. the adsorption begins at the moment $t = 0$: $\eta(0,x,z) = 0$.

For the determination of $C(t,x,y,z)$ and $\eta_i(t,x,z)$, it is necessary to solve Eqs. (1) and (2) with the mentioned initial and boundary conditions, by using numerical methods. The number of adsorbed particles on the sites of the i^{th} type, $N_i(t)$, can be

determined by integration of $\eta_i(t,x,z)$ over the sensing element surface. If the contribution of a particle adsorption to the senor signal does not depend on the place on the sensing surface where the particle is bound, but only on the type of the adsorption site, the sensor response will depend on the numbers of adsorbed particles per each site type.

When the total sensor response is the sum of contributions of n components, of which each is the product of the number of adsorbed particles of a given component, $N_i(t)$, and the corresponding weight factor w_i (i = 1, 2, ... , n), the temporal response is

$$R = w_1N_1 + w_2N_2 + \ ... \ + w_nN_n \tag{4}$$

The weight factor w_i equals the average contribution of a single adsorbed particle of the i^{th} component to the sensor response. However, for some types of adsorption-based sensors, the response can be represented by the simpler expression

$$R = w\sum_{i=1}^{n} N_i \tag{5}$$

For instance, in the case of resonant micro/nanocantilevers and acoustic wave mechanical sensors, particle adsorption changes the mass of the mechanical sensing structure, so that w is determined by the mass of a single analyte particle, thus it is independent on the type of the site where the particle was adsorbed. Also, in the case of plasmonic sensors, it is reasonable to assume that the mean refractive index change when an analyte particle is adsorbed is $w = (n_a\text{-}n_e)/N_{max}$, where n_a is the refractive index value of the analyte, n_e is the refractive index of the surrounding medium, and N_{max} is the total number of adsorption sites on the surface [42]. In these cases, it is justified to use Eq. (5).

Numerical solving of Eqs. (1) and (2) requires the surface distributions of different adsorption sites to be known, which is rarely the case. Instead of that, approximations can be introduced in order to simplify the equations, which can even enable obtaining of the analytical solution valid for the transient regime and/or the steady state. The approximations are introduced based on the comparison of adsorption, convection and diffusion time scales.

2.2 Adsorption limited response kinetics

A significant reduction of mathematical complexity of the problem is possible when it is justified to assume that the concentration of the analyte in the reaction chamber is spatially uniform, constant in time, and equal to the concentration in the sample injected in the chamber. Eq. (3) is then reduced to $C(t,x,y,z) = C_0 = \text{const}$. The spatial independence of the concentration C_o and $\eta_{max,i}$ implies the uniformity of the surface density of adsorbed particles η_i on the surface S_i, so the number of particles adsorbed on sites of the i^{th} type is $N_i = \eta_i A_i$. The number of adsorption sites of that type is $N_{max,i} = \eta_{max,i}A_i = \nu_i N_{max}$, where ν_i is introduced as a measure of abundance of these sites in the total number of sites on the sensing surface, N_{max}. The model of the multicomponent AD process of a single analyte on the surface with n types of adsorption sites, derived from Eqs. (2), is therefore represented by the set of n mutually independent equations

$$\frac{dN_i}{dt} = k_{ai}C_o(N_{\max,i} - N_i) - k_{di}N_i = a_i - d_i, i = 1, 2, \ ... \ , n \tag{6}$$

The analytical solution of each of Eqs. (6), with the initial condition $N_i(0) = 0$, is

$$N_i(t) = \frac{k_{ai}C_0}{k_{di} + k_{ai}C_0} N_{\max,i}\left(1 - e^{-(k_{di}+k_{ai}C_0)t}\right) = N_{ie}\left(1 - e^{-t/\tau_{AL,i}}\right) \tag{7}$$

where N_{ie} is the number of adsorbed particles in the steady state, which establishes with the time constant of the AD process, $\tau_{AL,i}$. For the steady state $dN_i/dt = 0$, i.e. $a_i = d_i$. The sensor response is determined by Eq. (4) or Eq. (5).

This model is applicable in the cases where the transfer flux toward the sites of each type is sufficiently greater than the adsorption flux, so that the binding kinetics is adsorption limited [31, 32, 37]. This means that the number of adsorbed particles on the given surface and at the given analyte concentration is determined only by the AD process parameters at any given time. This is the ideal case for obtaining the data about the AD process and its kinetics from the measured time response of the sensor. The transport-adsorption regime of this kind is typical for fast diffusing particles (such as gas molecules and certain biomolecules of small mass).

2.3 Mass transfer influenced response kinetics

When the transport flux of analyte particles is lower than the adsorption flux, or comparable with it, the time evolution of the numbers of adsorbed particles is affected by mass transfer processes [31, 32, 37]. The temporal and spatial change of the analyte concentration in the sensor chamber depends on the parameters of AD and mass transfer processes in the system of a given geometry. As the adsorption flux becomes more dominant, the change of the analyte concentration in the chamber becomes more pronounced due to the slow compensating influx of particles carried by transport processes in the space that is being depleted of particles due to their fast binding to the adsorbing surface. Here, the analysis will be focused on the situation in which a thin depleted layer is formed adjacent to the sensing surface, because it is common in many types of microfluidic sensors (especially those whose reaction chamber height is of the order of ≥10 μm [43]). It also enables approximations to be used, which lead to the simplified time response mathematical model, and also yield the analytical expression for the AD noise spectral density.

When the diffusion time scale is greater than the convection time scale (expressed by $h_c^2/D > L_c/v_m$, where v_m is the mean convection velocity), not all the particles from the chamber volume can participate in the adsorption process, but only those from the layer of a certain thickness adjacent to the adsorbing surface. If the thickness of that layer is small compared to the chamber height and the length of the adsorbing zone, the temporally and spatially variable analyte concentration in the chamber can be approximated by the two-compartment model (TCM), whose applicability is experimentally confirmed [31, 44, 45]. According to that model, the chamber can be divided into two parts (compartments). One of them is the inner compartment, which is adjacent to the adsorbing surface, and contains a variable analyte concentration due to the depletion of analyte particles. The other, outer compartment, contains the analyte at the same concentration as it is in the sample injected in the chamber, C_0. Also, according to the model, all quantities are averaged over the adsorbing surface, and the transport between the two compartments is described by the mass transfer coefficient, k_m. It is assumed that the zones S_i (with binding sites of the type i) consist of a multitude of smaller areas scattered over the sensing surface (as illustrated in **Figure 1** (right)), so that different adsorption sites are mixed. The averaging of quantities over the sensing surface can thus approximate the actual conditions with sufficient accuracy, making the use of TCM justified. Furthermore, the model equates the rate of change of the total

number of adsorbed particles with the net number of particles that enter the inner compartment in unit time, i.e.

$$\frac{dN}{dt} = k_m A(C_0 - C_{s,TCM}) \tag{8}$$

where the mass transfer coefficient is given as $k_m = 1.467(D^2 v_m/(L_s h_c))^{1/3}$ [31]. Since the total number of particles adsorbed on the entire sensing surface equals

$$N = \sum_{i=1}^{n} N_i, \tag{9}$$

and Eqs. (2) after averaging of the quantities over the surface yield

$$\frac{dN_i}{dt} = k_{ai} C_{s,TCM}(N_{\max,i} - N_i) - k_{di} N_i = a_{eff,i} - d_{eff,i} \ (i = 1, 2, \ldots, n), \tag{10}$$

Eqs. (8)–(10) imply that the analyte concentration adjacent to the adsorbing surface is determined by the expression

$$C_{s,TCM} = \frac{C_0 + \sum_{k=1}^{n} k_{dk} N_k/(k_m A)}{1 + \sum_{k=1}^{n} k_{ak}(N_{\max,k} - N_k)/(k_m A)} \tag{11}$$

The time evolution of the numbers of adsorbed particles on different types of sites is determined by Eqs. (10) and (11), i.e. by $n + 1$ coupled equations. This system of equations is significantly simpler than the starting system (Eqs. (1) and (2)), and can be efficiently solved by using numerical methods for the given initial conditions. The sensor response is then determined by Eq. (4) or (5). The steady-state values of the numbers of adsorbed particles are obtained from Eqs. (10) for $dN_i/dt = 0$, and they are the same as in the case of adsorption-limited regime

$$N_{ie} = \frac{k_{ai} C_0}{k_{di} + k_{ai} C_0} N_{\max,i}, i = 1, 2, \ldots, n. \tag{12}$$

The presented mathematical model is applicable for the thin depleted zone adjacent to the sensing surface, which is more likely to exist at lower D values, higher h_c, and faster convection. The analysis of Eq. (11) shows that at

$$k_m A >> \sum_{k=1}^{n} k_{ak} N_{\max,k} \tag{13}$$

$C_{s,TCM} \approx C_0$, so the model given by Eq. (10) reduces to the model that is valid in the case of adsorption-limited binding (Eq. (6)). Therefore, Eq. (13) is the condition for the transfer flux to dominate over the adsorption flux (while the diffusion is slow compared to the convection). When the condition (13) is not satisfied, it is necessary to use the mathematical model given by Eqs. (10) and (11) for the response analysis of sensors in which a thin depleted zone is formed. Based on these considerations, it can be concluded that the equations obtained by using TCM have broader applicability than expected: they are valid both for mass-transfer influenced and for adsorption-limited (the case of sufficiently high k_m, according to Eq. (13)) binding kinetics.

The simplest heterogeneous sensing surface contains two types of adsorption sites. The corresponding equations are

$$\frac{dN_i}{dt} = k_{ai}\frac{C_0 + (k_{d1}N_1 + k_{d2}N_2)/k_mA}{1 + [k_{a1}(N_{m1} - N_1) + k_{a2}(N_{m2} - N_2)]/k_mA}(N_{mi} - N_i) - k_{di}N_i$$
$$= a_{eff,i} - d_{eff,i} \tag{14}$$

where i equals 1 or 2.

3. Mathematical models of adsorption-desorption noise

Due to the inherently stochastic nature of processes involved in the analyte particle binding-unbinding events on the sensing surface, the number of adsorbed particles randomly fluctuates, even after reaching the steady state, so it can be expressed as

$$N = N_e + \Delta N \tag{15}$$

where ΔN denotes fluctuations. The fluctuations of the number of adsorbed particles, $\Delta N(t)$, result in the fluctuations of the sensor's time response, $\Delta R(t)$, which constitute the inevitable adsorption–desorption (AD) noise. Based on Eq. (4), these fluctuations are related as

$$\Delta R = \sum_{i=1}^{n} w_i \Delta N_i, \tag{16}$$

assuming n AD processes on the sensing surface, where ΔN_i denote the fluctuations of the number of particles that participate in the i^{th} AD process.

Here, the goal is to obtain the analytical expression for the spectral density of sensor AD noise, when all the transient processes are finished, i.e. when an steady state is established. According to Eq. (16), the basis of this analysis is the analysis of fluctuations of the number of adsorbed particles around the steady-state values. Before presenting the theoretical models of AD noise of sensors with heterogeneous sensing surface, a short overview will be given of the already published results that include mathematical modeling of AD noise of sensors and other micro/nanodevices.

An insight into the existing literature shows that AD noise analyses have been usually limited to the consideration of individual phenomena pertinent to fluctuations of the number of adsorbed particles – e.g. fluctuations originating from a stochastic single-analyte AD process [46] or fluctuations due to surface diffusion of adsorbed particles [47].

First papers on AD noise in micro/nanodevices were focused on resonant mechanical structures [12, 48, 49]. Dating from the same period is the first paper on AD fluctuations in micro-biosensors [13]. In subsequent publications, the analysis of AD fluctuations was performed for various types of sensors (mass sensors with micro/nanocantilevers [15, 16, 50], semiconductor resistive gas sensors [51], plasmonic sensors [52], quartz crystal microbalance gas sensors [19]), which operate in a single-gas environment, assuming Langmuir adsorption. In [53] a theoretical AD noise model is presented for the Wolkenstein adsorption of particles of a single gas, applicable in the case of chemical adsorption in semiconductor resistive sensors.

In real situations, certain processes (e.g. various cases of non-specific adsorption, or mass transfer processes), which are coupled with the AD process of target

particles, affect the sensor response, and thus influence the response fluctuations. Therefore, it is necessary for the AD noise analysis to include the coupling of multiple processes, depending on the considered practical case. In [54] the expression is derived for the PSD of adsorbed mass fluctuations due to the coupled AD processes of an arbitrary number of gases, by using the Langevin approach. The AD noise model in the case of multilayer adsorption according to the BET model is presented in [55, 56]. Analyte diffusion within the sensor chamber is considered together with the binding of particles to the surface sites, in order to analyze the fluctuations and noise figures of merit of biosensors in [14, 57] assuming the adsorption surface of infinite capacity. The coupling of mass transfer (convection and diffusion) and AD processes of one or multiple substances on the sensing surface is taken into account in the development of the AD noise model of microfluidic sensors, which is presented in [58–60]. The combined effect of the AD process, the mass transfer in the sensor chamber and the surface diffusion on the fluctuations of the number of adsorbed particles is analyzed in [61], and a good match is shown between the derived PSD of AD noise and the experimental results obtained by using a graphene gas sensor [62]. The influence of the analyte depletion from the sample on the AD noise is modeled and analyzed in [63]. In [64] the analysis is presented of the signal-to-noise ratio of a nanowire biosensor, based on stochastic simulations of the AD process coupled with diffusion.

According to the current trends in micro- and nanosensor development (the decrease of the sensing surface area, and the decrease of detectable concentrations), the analysis of AD fluctuations becomes increasingly significant for the estimation of limiting performances of such devices, and for optimization of sensor design and experimental methods. In spite of that, the topic of AD noise is scarce in the literature, compared to the total number of papers on chemical and biological sensors. Also, the published experimental results pertinent to AD noise are very scarce, and can be found for gas sensors [17–20].

In the following part of this Section, mathematical models will be presented that take into account the existence of different types of adsorption sites on the sensing surface.

3.1 Langevin method for multicomponent stochastic processes

There are two approaches that are commonly used for the analysis of the fluctuations of the number of adsorbed particles: the first is based on the master equation, and the second on the Langevin equation, with the use of Wiener-Khinchin theorem. Both the approaches are described in detail in Supplementary data of Ref. [59] for a competitive AD process of two analytes, and all the given expressions can be generalized in a simple manner in order to be valid for n-component AD processes, where $n \geq 2$. Here, the Langevin method will be presented, which enables efficient determination of the analytical expression for the power spectral density (PSD) of the sensor response fluctuation, starting from the kinetic macroscopic equations that describe a multicomponent stochastic process.

When adsorption and desorption processes occur on the heterogeneous active surface of a sensor, the number of particles adsorbed on each type of adsorption sites stochastically fluctuates in time. The fluctuations of the number of particles adsorbed on sites belonging to the i^{th} type are denoted with ΔN_i ($i = 1, 2 \ldots n$). All these fluctuating processes, when observed together, constitute a single complex random process, which belongs to the class of multicomponent Markov "gain and loss" processes [65]. Fluctuations on one type of sites (ΔN_i) are a single component of that process. A complex process that has n ($n \geq 2$) components can be represented by an n-dimensional column vector $\mathbf{\Delta N} = [\Delta N_1 \Delta N_2 \ldots \Delta N_n]^{\mathbf{T}}$

(the superscript "T" denotes matrix transposition). The Langevin equation expressed in the matrix form is then (Supplementary data of Ref. [59])

$$\frac{d(\Delta\mathbf{N}(t))}{dt} = -\mathbf{K}\cdot\Delta\mathbf{N}(t) + \boldsymbol{\xi}(t) \tag{17}$$

where $\boldsymbol{\xi}(t) = [\xi_1(t)\xi_2(t) \ldots \xi_n(t)]^{\mathbf{T}}$ is the vector of the Langevin source functions, and $\mathbf{K}$ is the square $n \times n$ matrix whose elements are determined by the process parameters that influence the dynamics of analyte particles binding-unbinding random events. Elements of this matrix will later be derived for each of the analyzed cases of adsorption on heterogeneous surfaces. The symbol "·" is the matrix multiplication operator.

The Langevin equation in the complex domain ($\omega = 2\pi f$, f being the Fourier frequency) yields

$$\Delta\mathbf{N}(\mathrm{j}\omega) = (\mathbf{K} + \mathrm{j}\omega\mathbf{I})^{-1}\cdot\boldsymbol{\xi}(\mathrm{j}\omega) \tag{18}$$

(where $\Delta\mathbf{N}(\mathrm{j}\omega) = [\Delta N_1(\mathrm{j}\omega)\ \Delta N_2(\mathrm{j}\omega)\ \ldots\ \Delta N_n(\mathrm{j}\omega)]^{\mathbf{T}}$, $\boldsymbol{\xi}(\mathrm{j}\omega) = [\xi_1(\mathrm{j}\omega)\xi_2(\mathrm{j}\omega) \ldots \xi_n(\mathrm{j}\omega)]^{\mathbf{T}}$, and $\mathbf{I}$ is the $n \times n$ unity matrix), and then the $n \times n$ matrix of single-sided power spectral and cross-spectral densities of the numbers of adsorbed particles, $\mathbf{S}^2{}_{\Delta\mathbf{N}}(\omega)$, whose elements are determined by the expression

$$\begin{aligned}\mathbf{S}^2_{\Delta\mathbf{N}}(\omega) &= <\Delta\mathbf{N}(\mathrm{j}\omega)\Delta\mathbf{N}^{\mathbf{T}}(-\mathrm{j}\omega)> \\ &= (\mathbf{K} + \mathrm{j}\omega\mathbf{I})^{-1}\cdot <\boldsymbol{\xi}(\mathrm{j}\omega)\cdot\boldsymbol{\xi}^{\mathbf{T}}(-\mathrm{j}\omega)> \cdot \left((\mathbf{K} - \mathrm{j}\omega\mathbf{I})^{-1}\right)^{\mathbf{T}} \\ &= (\mathbf{K} + j\omega\mathbf{I})^{-1}\cdot\mathbf{S}^2_{\boldsymbol{\xi}}\cdot\left(\mathbf{K}^{\mathbf{T}} - j\omega\mathbf{I}\right)^{-1}\end{aligned} \tag{19}$$

The expressions for the elements of the matrix $S_\xi{}^2$ can be derived by using the formal statistical approach, as presented in [66]. Here only the final result is shown (d_{ie} are the effective probabilities of increase or decrease of the number of adsorbed particles at sites of the i^{th} type in unit time)

$$S^2_{\xi,il} = \begin{cases} 4d_{ie}, & i = l \\ 0, & i \neq l \end{cases} \tag{20}$$

By using the Wiener-Khinchin theorem [67] and Eqs. (16) and (19) the expression is obtained for the PSD of the sensor response fluctuations [59], i.e. for the PSD of AD noise

$$\begin{aligned}S^2_{\Delta R}(\omega) &= \sum_{i=1}^{n}\sum_{k=1}^{n}\left(w_i w_k S^2_{\Delta N,ik}(\omega)\right) \\ &= \mathbf{W}\cdot\mathbf{S}^2_{\Delta\mathbf{N}}(\omega)\cdot\mathbf{W}^{\mathbf{T}} \\ &= \mathbf{W}\cdot(\mathbf{K} + j\omega\mathbf{I})^{-1}\cdot\mathbf{S}^2_{\boldsymbol{\xi}}\cdot\left(\mathbf{K}^{\mathbf{T}} - j\omega\mathbf{I}\right)^{-1}\cdot\mathbf{W}^{\mathbf{T}}\end{aligned} \tag{21}$$

where the row vector of weight factors $\mathbf{W} = [w_1\, w_2\ \ldots\ w_{\mathrm{n}}]$ is introduced.

3.2 Adsorption limited binding

In the case of the transport-adsorption regime, known as the rapid mixing regime, the transfer flux toward the adsorption sites dominates over the adsorption flux, so the dependence of the concentration on the spatial coordinates is negligible,

and it results in adsorption-limited response kinetics, determined by the kinetic Eqs. (6). These equations are mutually independent, and show the change of the number of adsorbed particles on any of n sites, in the form of the difference of the actual adsorption and desorption rates, a_i and d_i, which are linear functions of the number of adsorbed particles N_i (i = 1,2 ... n). The fluctuations can then be analyzed by directly applying the Langevin method. This approach is usually applicable in the case of AD process of gas particles. In other cases (e.g. in biological sensors, where the analyte particles are typically large macromolecules with slow diffusion in liquid samples) it is necessary to take into account the influence of transfer processes on the fluctuations of the number of adsorbed particles.

Eqs. (6) and (15) directly yield the system of n independent Langevin equations

$$\frac{d\Delta N_i}{dt} = -(k_{ai}C_o + k_{di})\Delta N_i + \xi_i, i = 1, 2, \ldots, n \tag{22}$$

after a random source function is added on the right side of each equation.

When this system of equations is written in the matrix form, as shown in SubSection 3.1, the quadratic diagonal matrix **K** is obtained, and its elements are

$$K_{il} = \begin{cases} k_{ai}C_o + k_{di}, & i = l \\ 0, & i \neq l \end{cases}, i = 1, 2, \ldots, n, l = 1, 2, \ldots, n \tag{23}$$

The elements of the matrix $\mathbf{S}^2_{\boldsymbol{\xi}}$ are (Eq. (20))

$$S^2_{\xi,il} = \begin{cases} 4k_{di}N_{ie}, & i = l \\ 0, & i \neq l \end{cases}, i = 1, 2, \ldots, n, l = 1, 2, \ldots, n \tag{24}$$

where N_{ie} is given by Eq. (7).

Since all the quadratic matrices on the right side of Eq. (19) are diagonal, the matrix $\mathbf{S}^2_{\Delta\mathbf{N}}(\omega)$ is also diagonal, i.e. the cross-spectral densities $S^2_{\Delta\mathbf{N},il}$ are equal to zero (the random processes ΔN_i and ΔN_l are statistically independent for every pair of i and l, $i \neq l$). The spectral densitities of fluctuations of the numbers of adsorbed particles are of the Lorenzian type

$$S^2_{\Delta N,ii}(f) = \frac{4k_{di}N_{ie}\tau^2_{AL,i}}{1 + (2\pi f)^2\tau^2_{AL,i}} \tag{25}$$

with the characteristic frequency $f_{c,AL,i} = 1/(2\pi\tau_{AL,i})$, where $\tau_{AL,i} = k_{ai}C_0 + k_{di}$, and the AD noise PSD of a sensor with n types of adsorption sites is determined by the sum of Lorenzians

$$S^2_{\Delta R}(f) = \sum_{i=1}^{n} w_i^2 S^2_{\Delta N,ii}(f) = \sum_{i=1}^{n} w_i^2 \frac{4k_{di}N_{ie}\tau^2_{AL,i}}{1 + (2\pi f)^2\tau^2_{AL,i}} \tag{26}$$

3.3 Mass transfer influenced binding

The use of TCM for approximation of spatially and temporally dependent analyte concentration in a sensor chamber (see SubSection 2.3) has enabled the presentation of the macroscopic kinetic equations (Eqs. (10), (11) and (14)) in the form in which the change of the number of adsorbed particles in unit time equals the difference between the instantaneous effective rates of adsorption and desorption, $a_{eff,i}$ and $d_{eff,i}$, which are explicitely dependent only on the instantaneous

numbers of adsorbed particles on adsorption sites of all types. Such form of the equations is suitable for fluctuation analysis. In order for the Langevin method to be applicable for obtaining the PSD of fluctuations of a sensor response when coupling of complex (n-component) AD process and mass transfer is considered, a linear approximation of the functions $a_{eff,i}$ and $d_{eff,i}$ around the equilibrium values of the numbers of adsorbed particles is used (assuming small fluctuations relative to the equilibrium values, $\Delta N_i << N_{ie}$) [59, 66]

$$a_{eff,i} \approx a_{eff,i}(N_{1e}, N_{2e} \ldots N_{ne}) + \sum_{k=1}^{n} \left(\left. \frac{\partial a_{eff,i}}{\partial N_k} \right|_e \cdot \Delta N_k \right) \tag{27}$$

$$d_{eff,i} \approx d_{eff,i}(N_{ie}) + \left. \frac{\partial d_{eff,i}}{\partial N_i} \right|_e \cdot \Delta N_i \tag{28}$$

All the derivatives are calculated for $N_1 = N_{1e}$, $N_2 = N_{2e}$ ... $N_n = N_{ne}$ (the equilibrium values are determined by Eq. (12)), which is in the above expressions denoted with the subscript "e" within the derivatives. It can be noticed that $a_{eff,i}(N_{1e}, N_{2e} \ldots N_{ne}) = d_{eff,i}(N_{ie})$, since the adsorption and desorption rates are pertinent to the equilibrium state, according to the condition $dN_i/dt = 0$. By substituting Eqs. (27) and (28) into Eqs. (10), linearized kinetic equations are obtained, which, after the addition of Langevin source functions on their right side assume the form of Langevin equations, shown by the matrix Eq. (17). The obtained expressions imply that the elements of the quadratic matrix **K** are

$$K_{il} = \begin{cases} -\left(\left. \frac{\partial a_{eff,i}}{\partial N_i} \right|_e - \left. \frac{\partial d_{eff,i}}{\partial N_i} \right|_e \right), & i = l \\ -\left. \frac{\partial a_{eff,i}}{\partial N_l} \right|_e, & i \neq l \end{cases}, i = 1, 2, \ldots, n, l = 1, 2, \ldots, n \tag{29}$$

and after differentiation

$$K_{ii} = \frac{k_{ai}C_0 + k_{di} + \left(k_{ai} \sum\limits_{\substack{k=1 \\ k \neq i}}^{n} k_{dk}N_{ek} + k_{di} \sum\limits_{\substack{k=1 \\ k \neq i}}^{n} k_{ak}(N_{\max,k} - N_{ek}) \right) / (k_m A)}{1 + \sum\limits_{k=1}^{n} k_{ak}(N_{\max,k} - N_{ek}) / (k_m A)} \tag{30}$$

$$K_{ij} = -\frac{k_{ai}}{k_m A} \frac{k_{aj}C_0 + k_{dj} + \left(k_{aj} \sum\limits_{k=1}^{n} k_{dk}N_{ek} + k_{dj} \sum\limits_{k=1}^{n} k_{ak}(N_{\max,k} - N_{ek}) \right) / (k_m A)}{\left(1 + \sum\limits_{k=1}^{n} k_{ak}(N_{\max,k} - N_{ek}) / (k_m A) \right)^2} (N_{\max,i} - N_{ei}) \tag{31}$$

Based on Eq. (20)

$$S^2_{\xi,il} = \begin{cases} 4k_{di}N_{ie}, & i = l \\ 0, & i \neq l \end{cases}, i = 1, 2, \ldots, n, l = 1, 2, \ldots, n \tag{32}$$

Now, all the quantities are known that enable the determination of the spectral and cross-spectral densities of fluctuations of the numbers of adsorbed particles on different types of adsorption sites, according to Eq. (19), as well as the spectral density of the sensor response fluctuations, based on Eq. (21)

When there are two types of adsorption sites on the sensing surface, the elements of the matrices **K** and $\mathbf{S}^2_{\xi}$ are, according to Eqs. (30)–(32)

$$K_{ii} = \frac{k_{ai}C_0 + k_{di} + \left(k_{ai}k_{dj}N_{ej} + k_{di}k_{aj}\left(N_{\max,j} - N_{ej}\right)\right)/(k_mA)}{1 + (k_{a1}(N_{\max,1} - N_{e1}) + k_{a2}(N_{\max,2} - N_{e2}))/(k_mA)}, i = 1,2, j = 1,2.$$

$$K_{ij} = -\frac{k_{ai}}{k_mA}\frac{k_{aj}C_0 + k_{dj} + \left(k_{aj}k_{dj}N_{\max,j} + k_{aj}k_{di}N_{ei} + k_{dj}k_{ai}(N_{\max,i} - N_{ei})\right)/(k_mA)}{\left(1 + \sum_{k=1}^{n} k_{ak}(N_{\max,k} - N_{ek})/(k_mA)\right)^2}(N_{\max,i} - N_{ei})$$

$$\mathbf{S}^2_{\xi} = \begin{bmatrix} 4k_{d1}N_{e1} & 0 \\ 0 & 4k_{d2}N_{e2} \end{bmatrix}$$

so the PSD of the AD noise, calculated based on Eq. (21), is

$$S^2_{\Delta R}(f) = 4\left(w_1^2k_{d1}N_{e1} + w_2^2k_{d2}N_{e2}\right)\frac{\tau^2_{MT,1}\tau^2_{MT,2}}{\tau^2_{Mt,3}}\frac{1 + (2\pi f)^2\tau^2_{MT,3}}{\left(1 + (2\pi f)^2\tau^2_{MT,1}\right)\left(1 + (2\pi f)^2\tau^2_{MT,2}\right)} \tag{33}$$

where

$$\tau_{MT,1,2} = 2\left[K_{11} + K_{22} \pm \sqrt{(K_{11} - K_{22})^2 + 4K_{12}K_{21}}\right]^{-1} \tag{34}$$

$$\tau_{MT,3} = \sqrt{\left(w_1^2d_{1e} + w_2^2d_{2e}\right)\left[(w_1K_{22} - w_2K_{21})^2d_{1e} + (w_2K_{11} - w_1K_{12})^2d_{2e}\right]^{-1}} \tag{35}$$

The characteristic frequencies of the AD noise spectrum are $f_{c,\mathrm{MT},i} = 1/(2\pi\tau_{MT,i})$, where i is 1, 2 or 3.

The expressions for K_{ii} and K_{ij} for a fast mass transfer (at suffuciently high k_m) become approximately equal to the expressions given by Eq. (23), which are valid for the case of adsorption-limited binding. Also, in that case, Eq. (33) reduces to Eq. (26) for $n = 2$. This demonstrates a wider applicability of the expressions derived by using TCM. Namely, when the zone adjacent to the sensing surface, which contains the analyte particles that can participate in the adsorption is narrow, the expressions derived by using TCM for mass transfer influenced binding are valid even in the case of high k_m values, when the binding is adsorption limited.

4. Results and discussion

In order to analyze the effects of mass transfer and surface heterogeneity on the sensor temporal response and AD noise, numerical calculations are performed for the case of protein biosensor, on whose active surface two types of adsorption sites exist with different affinities toward the target analyte. The results are presented in terms of the adsorbed mass on the sensing surface, assuming the values of adsorption and desorption rate constants from the ranges corresponding to biomolecules and biosensors [68]: $k_{a1} = 1.3{\cdot}10^{-18}$ m^3/s, $k_{d1} = 0.4$ 1/s, $k_{a2} = 1.3{\cdot}10^{-20}$ m^3/s and $k_{d2} = 0.02$ 1/s, the mass of a single analyte particle $w = 20$ kDa, and the total of $N_{max} = 10^8$ adsorption sites on the sensing surface of area $A = 10^{-9}$ m^2. The analyte concentration is $C_0 = 5{\cdot}10^{17}$ 1/m^3.

Figure 2 shows the temporal change of adsorbed mass, representing the temporal response of the sensor whose measured parameter is a function of the total bound mass of the target protein. The total mass adsorbed on the sensing surface is

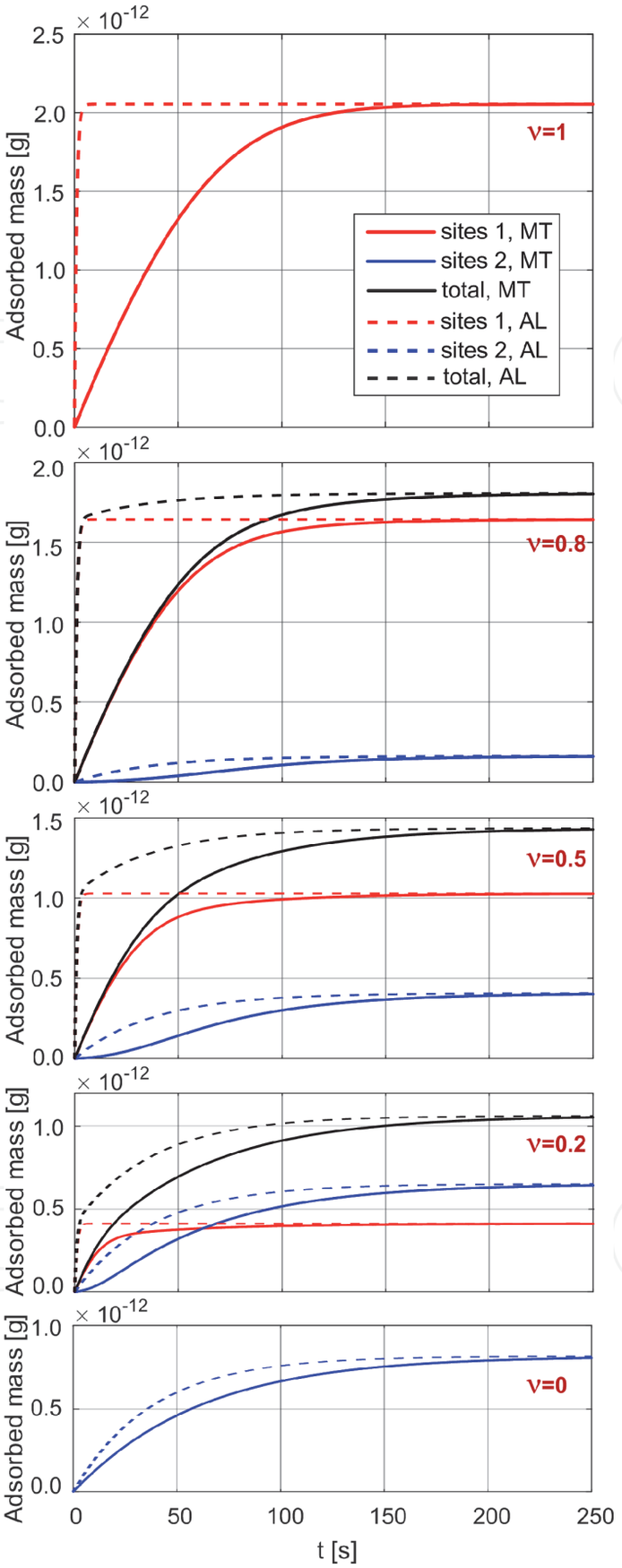

Figure 2.
The temporal change of the total adsorbed mass (black lines) on the heterogeneous surface of a biosensor. The adsorbed mass on each type of adsorption sites are also shown (red and blue lines). The five diagrams correspond to different shares of the types of adsorption sites in the overall number of sites, which is expressed by different values of the parameter ν, where $N_{max,1} = \nu N_{max}$ *and* $N_{max,2} = (1-\nu)N_{max}$. *The solid-line curves represent "slow" mass transfer (denoted as "MT"), and the dashed-line curves represent adsorption- limited kinetics (denoted as "AL").*

shown (black lines), as well as the adsorbed amounts on each of the two types of adsorption sites (red lines for the type 1 sites, blue lines for the type 2 sites). The five diagrams correspond to different shares of the types of adsorption sites in the overall number of sites, which is expressed by different values of the parameter ν (1; 0.8; 0.5; 0.2, 0), where $N_{max,1} = \nu N_{max}$ and $N_{max,2} = (1\text{-}\nu)N_{max}$. Different cases are illustrated: from the presence of only the high-affinity sites (type 1 sites), to various ratios of the numbers of sites belonging to the two types ($N_{max,1}$:$N_{max,2}$ that equals 4:1, 1:1 and 1:4), and, finally, to the presence of only the low-affinity sites (type 2 sites) on the sensing surface. As the measure of the affinity, the affinity constant is used, which is defined by the ratio k_{ai}/k_{di}. The curves are obtained by computer simulation, based on the model that takes into account the mass transfer effects (Eqs. (14)), for two values of the mass transfer coefficient: $k_{m\mathrm{I}} = 2{\cdot}10^{-3}$ m/s (solid line) and $k_{m\mathrm{II}} = 9{\cdot}10^{-1}$ m/s (dashed line). For $k_m > k_{m\mathrm{II}}$, the obtained curves overlap with those for $k_{m\mathrm{II}}$, and they also overlap with the curves obtained by the use of the model that neglects mass transfer (Eqs. (6) and (7)). This means that the value of $k_{m\mathrm{II}}$ is high enough for the influence of mass transfer on the sensor's temporal response to be considered as negligible, so that conclusions about the mass transfer influence can be made by comparing the responses for $k_{m\mathrm{I}}$ and $k_{m\mathrm{II}}$.

In the absence of the mass transfer influence (dashed-line curves shown in the diagram), the existence of two types of adsorption sites is clearly noticeable based on the sharp transition from fast to slow transient regime (for ν equal to 0.8, 0.5 or 0.2). The time evolution of the total adsorbed mass is rapid at first, as it is dominantly determined by adsorption on the higher affinity sites, with the time constant of approximately 1 s, but it then slowly approaches the steady state, with the time constant of approximately 38 s (AD process on sites of lower affinity). Even with a lower share of low affinity sites, the AD process occurring on them determines the sensor response rate. Different shares of the two types of adsorption sites influence the sensor response value in the steady state.

When the mass transfer is characterized by $k_{m\mathrm{I}}$, a pronounced MT influence on the sensor response kinetics is evident at all values of ν. Such results are in accord with Eq. (13) by which the analytic criterion is defined for a negligible influence of MT on the response. For two types of adsorption sites, that criterion is $k_m >> k_{mg}$, where $k_{mg} = (k_{a1}{\cdot}\nu + k_{a2}{\cdot}(1\text{-}\nu)){\cdot}N_{max}/A$, and for the given parameters k_{mg} equals $1.3{\cdot}10^{-1}$ m/s, $1{\cdot}10^{-1}$ m/s, $6.6{\cdot}10^{-2}$ m/s, $2.7{\cdot}10^{-2}$ m/s, and $1.3{\cdot}10^{-3}$ m/s for ν equal to 1, 0.8, 0.5, 0.2 and 0, respectively. Hence, when $k_m = k_{m\mathrm{I}}$, the above-mentioned condition is not satisfied for any ν. It can be seen that the minimal MT coefficient value at which the response kinetics can be considered as adsorption limited increases with the increase of the type 1 sites share. The influence of mass transfer characterized by the parameter $k_{m\mathrm{I}}$ on the time evolution of the number of adsorbed particles is more pronounced for the sites with a higher adsorption rate constant. Thus, the initial evolution of the total number of adsorbed particles is much slower compared to the case of adsorption limited binding.

Figure 3 shows the spectral density (SD) of adsorbed mass fluctuations, $(S_{\Delta R}{}^2(f))^{1/2}$, i.e. the spectral density of sensor AD noise, for the same parameter values for which the response shown in **Figure 2** was obtained. It is obtained as a square root of the PSD, given by Eq. (33), which, apart from surface heterogeneity, takes into account mass transfer. SDs of the total adsorbed mass are shown for two values of the MT coefficient: $k_{m\mathrm{I}} = 2{\cdot}10^{-3}$ m/s (solid red lines) and $k_{m\mathrm{II}} = 9{\cdot}10^{-1}$ m/s (solid blue lines), for each of five values of ν. As in the case of response, the curves obtained for $k_m > k_{m\mathrm{II}}$ match those for $k_{m\mathrm{II}}$. Also matching with them are the curves obtained by using Eq. (26), i.e. the model that neglects mass transfer. According to that model, PSD of AD noise equals the sum of PSDs of fluctuations of adsorbed masses on two types of sites. The SDs corresponding to these components are also

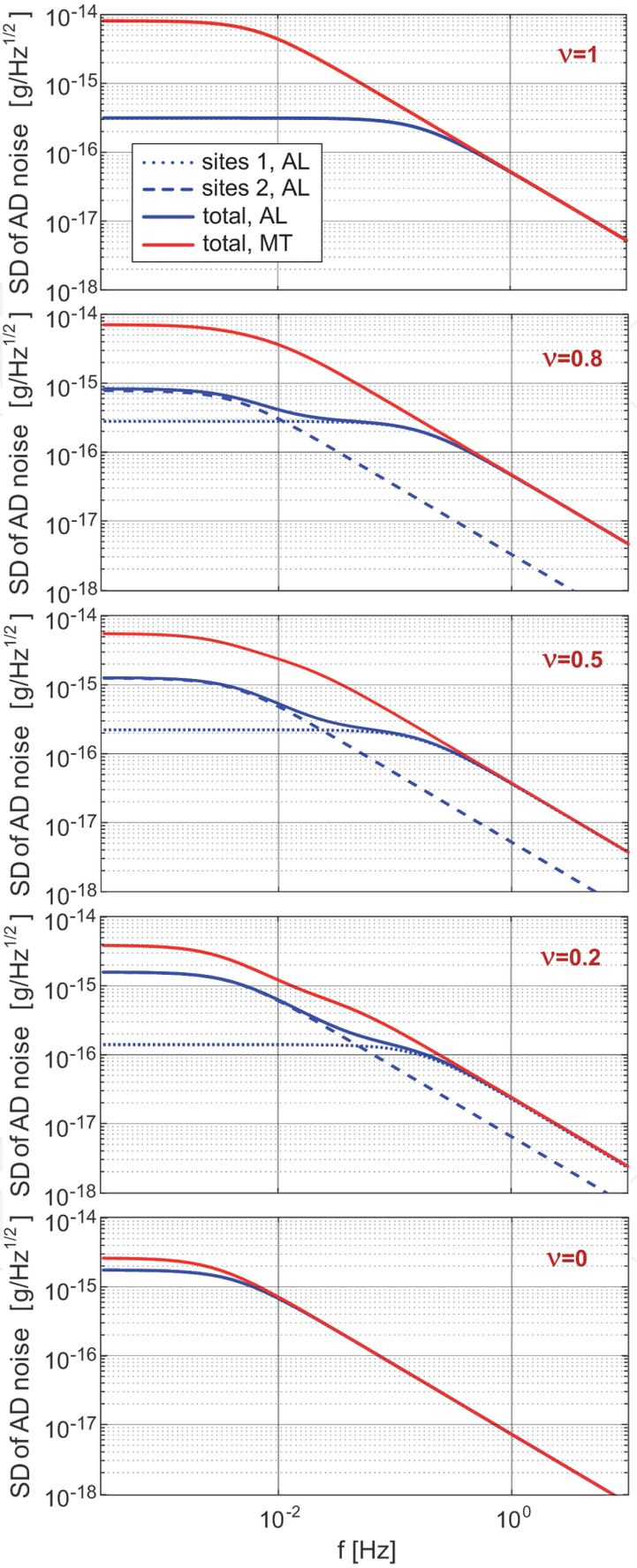

Figure 3.
The spectral density (SD) of adsorbed mass fluctuations, i.e. the spectral density of biosensor AD noise, for the same parameter values for which the response shown in ***Figure 2*** *was calculated. The total adsorbed mass SDs are shown for the cases when the mass transfer influence is pronounced (solid red lines), and when it is negligible (solid blue lines), for each of the five values of ν. Also shown are SDs of fluctuations of adsorbed masses on two types of sites (dotted lines denote type 1 sites, and dashed lines denote type 2 sites) in the absence of the mass transfer influence.*

shown in the diagrams (dotted lines denote type 1 sites, and dashed lines denote type 2 sites). Hence, the influence of mass transfer on the AD noise is negligible for $k_m = k_{m\mathrm{II}}$, and the comparison of the results for the shown SDs of total fluctuations for a given ν enables making conclusions on the influence of mass transfer on the sensor AD noise.

It can be noticed that at all the values of ν, mass transfer leads to the increase of the AD noise magnitude in the part of the spectrum where the characteristic frequencies belong. It also increases the AD noise (obtained by integration of the AD noise SD in the frequency range of interest), and thus influences the fundamental detection and quantification limits of a biosensor. For a given ν, mass transfer also causes a shift of the characteristic frequencies of the AD noise spectrum. Thus, the AD noise spectral analysis can yield information not only on adsorption and desorption rate constants and analyte concentration, but also on mass transfer parameters.

By comparing the diagrams for the case of a surface containing a single type of adsorption sites (i.e. for $\nu = 1$ or $\nu = 0$) with the diagrams for the sensors with a heterogeneous adsorbing surface (i.e. when ν equals 0.8, 0.5 or 0.2), it is obvious that the latter diagrams may exhibit a greater number of characteristic frequencies (three in the case of two type of adsorption sites), which can indicate the existence of different types of adsorption sites.

The diagrams also show that when the mass transfer influence is negligible, the two characteristic frequencies of the AD spectrum do not change at different shares of adsorption site types on the sensing surface. They are determined by the characteristic frequencies that correspond to the fluctuation spectra of adsorbed masses on each of site types, which are given by expressions $f_{c,AL,i} = 1/(2\pi\tau_{AL,i})$, where $\tau_{AL,i} = k_{ai}C_0 + k_{di}$, as given in Section 3.2. Contrary to that, when the mass transfer influence is pronounced, all the three AD noise spectrum characteristic frequencies change with ν, so that their values also contain the data on the share of a specific site type on the sensing surface. Therefore, as the parameters of all the processes and effects that influence the sensor temporal response are contained in the characteristic features of the AD noise spectrum, noise spectrum analysis can be used as an additional source of data in biosensing.

5. Conclusions

In this chapter, the mathematical modeling has been performed of time response and adsorption–desorption (AD) noise in microfluidic adsorption-based biosensors whose active surface is heterogeneous in the sense that it contains adsorption sites of different affinity toward the target analyte. The adsorption–desorption processes of analyte particles on different types of adsorption sites, as well as mass transfer in a microfluidic chamber, have been taken into account as the coupled processes that generate the sensor signal. The devised model of AD noise is the first that simultaneously takes into account surface heterogeneity and mass transfer through both the convection and diffusion of analyte particles. The analytical expression of the spectral density of AD noise has been derived. The models of the time response and AD noise of a sensor with heterogeneous adsorbing surface in the case of negligible mass transfer influence have also been presented. The criterion is given based on which it can be discerned whether the mass transfer influence is significant or negligible, so that the appropriate mathematical model of the response and noise can be chosen.

The derived mathematical models have been used for the analysis of the response and AD noise of protein biosensors that have two types of adsorption sites

on the sensing surface. The comparison of the results obtained by the use of the models that take into account mass transfer effects, and those that neglect them, for different shares of two types of binding sites, has enabled drawing conclusions on both separate and coupled influences of surface heterogeneity and transport processes on the sensor response and noise.

While a slow mass transfer increases the sensor response time, the existence of different adsorption site types affects both the transient regime and the sensor response magnitude in the steady state. The minimal mass transfer coefficient value at which the response kinetics can be considered as adsorption limited increases with the increase of the share of high affinity binding sites. The influence of mass transfer (of given parameters) on the time evolution of the number of adsorbed particles is more pronounced on sites with a higher adsorption rate constant.

At any share of the two types of binding sites on the sensing surface, mass transfer causes the increase of the AD noise, and thus increases the sensor's fundamental limits of analyte detection and quantification. For a given ratio of the numbers of adsorption sites of the two types, mass transfer causes a shift of the characteristic frequencies in the AD noise spectrum. When the mass transfer influence is pronounced, the characteristic frequencies shift with the change of the ratio of the numbers of sites of different types. Therefore, the AD noise spectrum analysis can yield information not only on adsorption and desorption rate constants and analyte concentration, but also on mass transfer parameters and on the share of a certain type of binding sites on the sensing surface. It can be used as an additional source of data in biosensing.

As the results of the performed analysis have shown a potentially significant influence of sensing surface heterogeneity and mass transfer processes on the sensor temporal response, as well as on AD noise, which is inevitable in adsorption-based sensors and determines their ultimate sensing performance, the presented mathematical models can enable better interpretation of measurement results, and give guidelines for ensuring lower noise levels and improved detection limits in microfluidic biosensors.

Acknowledgements

This research was funded by the Ministry of Education, Science and Technological Development of the Republic of Serbia, grant number 451-03-9/2021-2114/200026. It was also supported by the Science Fund of the Republic of Serbia, PROMIS, #6057070, Gramulsen.

Author details

Ivana Jokić
University of Belgrade – Institute of Chemistry, Technology and Metallurgy – National Institute of the Republic of Serbia, Belgrade, Serbia

*Address all correspondence to: ijokic@nanosys.ihtm.bg.ac.rs

IntechOpen

References

[1] Sackmann EK , Fulton AL, Beebe DJ. The present and future role of microfluidics in biomedical research. Nature. 2014;507: 181–189.

[2] Luka G, Ahmadi A, Najjaran H, Alocilja E, DeRosa M, Wolthers K, Malki A, Aziz H, Althani A, Hoorfar M. Microfluidics integrated biosensors: A leading technology towards lab-on-a-chip and sensing applications. Sensors. 2015;15: 30011–30031.

[3] Liu K-K, Wu R-G, Chuang Y-J, Khoo HS, Huang S-H, Tseng F-G. Microfluidic systems for biosensing. Sensors. 2010;10:6623–6661.

[4] Xua D, Huangc X, Guod J, Ma X. Automatic smartphone-based microfluidic biosensor system at the point of care. Biosensors and Bioelectronics. 2018;10:78–88.

[5] Srinivasan B, Tung S. Development and Applications of Portable Biosensors. Journal of Laboratory Automation. 2015; 20:365–389. doi.org/10.1177/2211068215581349

[6] Zu, Z.-H. Wang, N.-K. Chou, S. S. Lu, "A Wireless Bio-MEMS Sensor for C-Reactive Protein Detection Based on Nanomechanics", IEEE Internat. Conf. on Solid-State Circuits ISSCC 2006, San Francisco 2006, pp. 2298–2307.

[7] Padash M, Enz C, Carrara S. Microfluidics by Additive Manufacturing for Wearable Biosensors: A Review. Sensors. 2020;20:4236. doi: 10.3390/s20154236

[8] Nightingale AM, Leong CL, Burnish RA et al. Monitoring biomolecule concentrations in tissue using a wearable droplet microfluidic-based sensor. Nat. Commun. 2019;10:2741. https://doi.org/10.1038/s41467-019-10401-y

[9] Mejía-Salazar JR, Cruz KR, Vásques EMM, de Oliveira Jr. ON. Microfluidic Point-of-Care Devices: New Trends and Future Prospects for eHealth Diagnostics. Sensors. 2020,20: 1951. doi:10.3390/s20071951

[10] Mohd-Yasin F, Nagel DJ, Korman CE. Noise in MEMS. Meas. Sci. Technol. 2010;21:012001 1–22.

[11] Palasantzas G. Adsorption-desorption noise influence on mass sensitivity and dynamic range of nanoresonators with rough surfaces. J. Appl. Phys. 2007;101:076103 1–3.

[12] Djurić Z. Noise in Microsystems and Semiconductor Photodetectors. In: Proc. of the XLIV Conference ETRAN; 2000; Sokobanja. Serbia. 2000. p. 9–16.

[13] Arakelian VB, Wildt JR, Simonian AL. Investigation of stochastic fluctuations in the signal formation of microbiosensors. Biosensors and Bioelectronics. 1998.13:55–59.

[14] Hassibi A, Zahedi S, Navid R, Dutton RW, Lee TH. Biological shot-noise and quantum-limited signal-to-noise ratio in affinity-based biosensors. J. Appl. Phys. 2005.97:084701 1–10.

[15] Djurić Z, Jokić I, Frantlović M, Jakšić O. Influence of Adsorption-Desorption Process on Resonant Frequency and Noise of Micro- and Nanocantilevers. In: Proc. 23rd Internatinal Conference on Microelectronics (MIEL); 12–15 May 2002; Niš. Serbia. 2002. Vol. 2: p. 243–246.

[16] Kim S-J, Ono T, Esashi M. Study on the noise of silicon capacitive resonant mass sensors in ambient atmosphere. J. Appl. Phys. 2007;102:104304 1–6.

[17] Amin KR, Bid A. Effect of ambient on the resistance fluctuations of graphene. Appl. Phys. Lett. 2015;106:183105 1–5.

[18] Contaret T, Florido T, Seguin J-L, Aguir K. A Physics-Based Noise Model

for Metallic Oxide Gas Sensors Characterization. Procedia Engineering. 2011;25:375–378.

[19] Sedlak P, Sikula J, Majzner J, Vrnata M, Fitl P, Kopecky D, Vyslouzil F, Handel PH. Adsorption–desorption noise in QCM gas sensors. Sens. Actuators B: Chemical. 2012;166–167:264–268.

[20] Contaret T, Seguin J-L, Menini P, Aguir K. Physical-Based Characterization of Noise Responses in Metal-Oxide Gas Sensors. IEEE Sensors Journal. 2013;13:980–986. 10.1109/JSEN.2012.2227707

[21] Wang DS, Fan SK. Microfluidic Surface Plasmon Resonance Sensors: From Principles to Point-of-Care Applications. Sensors. 2016;16:1175. doi: 10.3390/s16081175

[22] Peña-Bahamonde J, Nguyen HN, Fanourakis SK, et al. Recent advances in graphene-based biosensor technology with applications in life sciences. J. Nanobiotechnol. 2018;16:75.

[23] Ambhorkar P, Wang Z, Ko H, Lee S, Koo K-in, Kim K, Cho D-il. Nanowire-Based Biosensors: From Growth to Applications. Micromachines. 2018;9:679. doi:10.3390/mi9120679

[24] Liu S, Guo X. Carbon nanomaterials field-effect-transistor-based biosensors. NPG Asia Mater. 2012;4:e23.

[25] Voiculescu I, Nordin AN. Acoustic wave based MEMS devices for biosensing applications. Biosensors and Bioelectronics. 2012;33:1–9.

[26] Zhang Y, LuoJ, Flewitt AJ, Cai Z, Zhao X. Film bulk acoustic resonators (FBARs) as biosensors: A review. Biosensors and Bioelectronics. 2018;116:1–15.

[27] Arlett JL, Myers EB, Roukes ML, Comparative advantages of mechanical biosensors. Nature Nanotechnology. 2011;6:203–215.

[28] Zheng F, Wang P, Du Q, Chen Y, Liu N. Simultaneous and Ultrasensitive Detection of Foodborne Bacteria by Gold Nanoparticles-Amplified Microcantilever Array Biosensor. Front. Chem. 2019;7:232.

[29] Mehand M, Srinivasan B, De Crescenzo G. Optimizing Multiple Analyte Injections in Surface Plasmon Resonance Biosensors with Analytes having Different Refractive Index Increments. Sci. Rep. 2015;5:15855. https://doi.org/10.1038/srep15855

[30] Schuck P, Zhao H. The role of mass transport limitation and surface heterogeneity in the biophysical characterization of macromolecular binding processes by SPR biosensing. Methods Mol. Biol. 2010;627:15–54. doi: 10.1007/978-1-60761-670-2_2.

[31] Myszka DG, He X, Dembo M, Morton TA, Goldstein B. Extending the Range of Rate Constants Available from BIACORE: Interpreting Mass Transport-Influenced Binding Data. Biophys. J. 1998;75:583–594.

[32] Gervais T, Jensen KF. Mass transport and surface reactions in microfluidic systems. Chem. Eng. Sci. 2006;61:1102–1121.

[33] Squires TM, Messinger RJ, Manalis SR. Making it stick: convection, reaction and diffusion in surface-based biosensors. Nature Biotechnology. 2008;26:417–426.

[34] Bishop J, Chagovetz AM, Blair S. Competitive displacement: A sensitive and selective method for the detection of unlabeled molecules. Optics Express. 2007;15:4390–4397.

[35] Karlsson R. Real-time competitive kinetic analysis of interactions between low-molecular-weight ligands in

solution and surface-immobilized receptors. Analytical Biochemistry. 1994;221:142–151.

[36] Tripathi S, Tabor RF. Modeling two-rate adsorption kinetics: Two-site, two-species, bilayer and rearrangement adsorption processes. Journal of Colloid and Interface Science. 2016;476:119–131.

[37] Jokić I, Radulović K, Frantlović M, Đurić Z, Vasiljević-Radović D. Combined influence of competitive binding and mass transfer on response of affinity-based biosensors. In: Proc. Regional Biophysics Conference; 3.-7 September 2012; Kladovo. Serbia. 2012. p. 45–47.

[38] Ding YX, Hlady V. Competitive Adsorption of Three Human Plasma Proteins onto Sulfhydryl-to-sulfonate Gradient Surfaces. Croat. Chem. Acta. 2011;84:193–202.

[39] Svitel J, Boukari H, Van Ryk D, Willson RC, Schuck P. Probing the Functional Heterogeneity of Surface Binding Sites by Analysis of Experimental Binding Traces and the Effect of Mass Transport Limitation. Biophysical Journal. 2007;92:1742–1758.

[40] Kumar KV, Gadipelli S, Wood B, Ramisetty KA, Stewart AA, Howard CA, Brett DJL, Rodriguez-Reinoso F. Characterization of the adsorption site energies and heterogeneous surfaces of porous materials. J. Mater. Chem. A. 2019;7:10101–10137.

[41] Andrić S, Tomašević-Ilić T, Bošković MV, Sarajlić M, Vasiljević-Radović D, Smiljanić MM, Spasenović M. Ultrafast humidity sensor based on liquid phase exfoliated graphene. Nanotechnology. 2020;32: 025505: 1–8.

[42] Choy TC. Effective Medium Theory: Principles and Applications. Oxford: Oxford University Press; 2015. https://doi.org/10.1093/acprof:oso/9780198705093.001.0001

[43] Gervais T. Mass transfer and structural analysis of microfluidic sensors [thesis]. Massachusetts Institute of Technology; 2006.

[44] Anderson H, Wingqvist G, Weissbach T, Wallinder D, Katardjiev I, Ingemarsson B. Systematic investigation of biomolecular interactions using combined frequency and motional resistance measurements. Sens. Actuators B: Chemical. 2011;153:135–144.

[45] Kusnezow W, Syagailo YV, Rüffer S, Klenin K, Sebald W, Hoheisel JD, Gauer C, Goychuk I. Kinetics of antigen binding to antibody microspots: Strong limitation by mass transport to the surface. Proteomics. 2006;6:794–803.

[46] Djurić Z. Mechanisms of noise sources in microelectromechanical systems. Microelectronics Reliability. 2000;40:919–932.

[47] Schmera G, Kish LB. Fluctuation-enhanced gas sensing by surface acoustic wave devices. Fluctuation and Noise Letters. 2002;2:L117–L123.

[48] Nguyen CT-C. Micromechanical resonators for oscillators and filters. In: Proc. IEEE Int. Ultrasonics Symposium; 7–10 November 1995; Seattle. WA. 1995. p. 489–499.

[49] Vig JR, Kim Y. Noise in microelectromechanical system resonators. IEEE Trans. Ultrason. Ferroelectr. Freq. Control. 1999;46: 1558–1565.

[50] Ekinci KL, Yang YT, Roukes ML. Ultimate limits to inertial mass sensing based upon nanoelectromechanical systems. J. Appl. Phys. 2004;95:2682–2689.

[51] Gomri S, Seguin J-L, Aguir K. Modelling on oxygen chemisorption induced noise in metallic oxide gas

sensors. Sens. Actuators B. 2005;107: 722–729.

[52] Jakšić Z , Đurić Z, Jakšić O, Jokić I, Frantlović M. Adsorption-desorption noise in surface plasmon resonance sensors. In: Proc. 8th International Conference on Fundamental and Applied Aspects of Physical Chemistry; 26–29 September 2006; Belgrade. Serbia. 2006. Vol. II: p. 671–673.

[53] Gomri S, Seguin J-L, Guerin J, Aguir K. Adsorption–desorption noise in gas sensors: Modelling using Langmuir and Wolkenstein models for adsorption. Sens. Actuators B: Chemical. 2006;114: 451–459.

[54] Djurić Z, Jokić I, Frantlović M, Jakšić O. Fluctuations of the number of particles and mass adsorbed on the sensor surface surrounded by a mixture of an arbitrary number of gases. Sensors and Actuators B: Chemical. 2007;127: 625–631. DOI: 10.1016/j. snb.2007.05.025

[55] Djurić ZG, Jokić IM, Frantlović MP, Radulović KT. Two-layer adsorption and adsorbed mass fluctuations on micro/nanostructures. Microelectronic Engineering. 2009;86:1278–1281.

[56] Djurić Z, Jokić I, Djukić I, Frantlović M. Fluctuations of the adsorbed mass and the resonant frequency of vibrating MEMS/NEMS structures due to multilayer adsorption. Microelectronic Engineering. 2010;87: 1181–1184.

[57] Hassibi A, Vikalo H, Hajimiri A. On noise processes and limits of performance in biosensors. J. Appl. Phys. 2007;102:014909 1–12.

[58] Jokić I, Djurić Z, Frantlović M, Radulović K, Krstajić P, Jokić Z. Fluctuations of the number of adsorbed molecules in biosensors due to stochastic adsorption-desorption processes coupled with mass transfer. Sensors and Actuators B: Chemical. 2012;166–167:535–543. http://dx.doi.org/10.1016/j.snb.2012.03.004

[59] Frantlović M, Jokić I, Djurić Z, Radulović K. Analysis of the Competitive Adsorption and Mass Transfer Influence on Equilibrium Mass Fluctuations in Affinity-Based Biosensors. Sensors and Actuators B: Chemical. 2013;189:71–79. doi:10.1016/j.snb.2012.12.080

[60] Jokić I, Frantlović M, Djurić Z, Radulović K, Jokić Z. Adsorption–desorption noise in microfluidic biosensors operating in multianalyte environments. Microelectronic Engineering. 2015;144:32–36. dx.doi.org/10.1016/j.mee.2015.02.032

[61] Djurić Z, Jokić I, Peleš A. Fluctuations of the number of adsorbed molecules due to adsorption-desorption processes coupled with mass transfer and surface diffusion in bio/chemical MEMS sensors. Microelectronic Engineering. 2014;124:81–85. http://dx.doi.org/10.1016/j.mee.2014.06.001

[62] Rumyantsev S, Liu G, Shur MS, Potyrailo RA, Balandin AA. Selective gas sensing with a single pristine graphene transistor. NanoLetters. 2012;12:2294–2295.

[63] Jokić I, Jakšić O. A second-order nonlinear model of monolayer adsorption in refractometric chemical sensors and biosensors: case of equilibrium fluctuations. Optical and Quantum Electronics. 2016;48:1–7. DOI: 10.1007/s11082-016-0620-0

[64] Tulzer G, Heitzinger C. Fluctuations due to association and dissociation processes at nanowire biosensor surfaces and their optimal design. Nanotechnology. 2015;26:025502 1–9.

[65] Van Kampen NG. Stochastic processes in physics and chemistry. Amsterdam: Elsevier BV; 1981–2007.

[66] Van Vliet CM. Macroscopic and microscopic methods for noise in devices. IEEE Trans. Electr. Dev. 1994; 41:1902–1915.

[67] Van der Ziel A. Fluctuation Phenomena in Semi-Conductors. London: Butterwrths; 1959.

[68] Canziani G, Zhang W, Cines D, Rux A, Willis S, Cohen G, Eisenberg R, Chaiken I. Exploring Biomolecular Recognition Using Optical Biosensors. Methods. 1999;19(2):253–269.